

Operational System for the Prediction of Tropical Cyclone Generated Winds and Waves

Andrew T. Cox and Vincent J. Cardone

Oceanweather Inc.
Cos Cob, CT

1. Introduction

It is well known that the details of the circulation of tropical cyclones are typically poorly resolved in surface wind analyses and forecasts produced by NWP centers. At many centers this shortcoming is addressed by a process of “bogussing” within a specified radius of the cyclone centers using solutions of simple parametric models. This paper describes an operational system used for determining inputs to a dynamical tropical wind field model and generation of tropical wind fields. The system is presently used for both hindcasting and real time global and regional wind and wave forecasting.

Sections 2 and 3 of this paper describe the tropical wind model and analysis/blending tool used in the generation of tropical cyclone winds. Section 4 is dedicated to the methodology used in determining inputs to the tropical wind model. A case study of Hurricane Floyd (1999) is presented in section 5, and is followed by a brief section on conclusions.

2. Tropical Wind Model

This model (TC96) was first developed into a practical tool in the Ocean Data Gathering Program (ODGP) (Cardone *et al.* 1976). It can provide a fairly complete description of time-space evolution of the surface winds in the boundary layer of a tropical cyclone. The model is an application of a theoretical model of the horizontal airflow in the boundary layer of a moving vortex. That model solves, by numerical integration, the vertically averaged equations of motion that govern a boundary layer subject to horizontal and vertical shear stresses. The equations are resolved in a Cartesian coordinate system whose origin translates at constant velocity, V_f , with the storm

center of the pressure field associated with the cyclone. Variations in storm intensity and motion are represented by a series of quasi-steady state solutions. The original theoretical formulation of the model is given by Chow (1971), a similar model was described more recently in the open literature by Shapiro (1983).

The version of the model applied in this paper is the result of two major upgrades, one described by Cardone *et al.* (1992) and the second by Cardone *et al.* (1994) and Thompson and Cardone (1996). The first upgrade mainly involved replacement of the empirical scaling law by a similarity boundary layer formulation to link the surface drag, surface wind and the model vertically averaged velocity components. The second upgrade added spatial resolution and generalized the pressure field specification. A more complete description of the theoretical development of the model as upgraded is given by Thompson and Cardone (1996).

The model pressure field is described as the sum of an axially symmetric part, and a large-scale pressure field of constant gradient. The symmetric part is described in terms of an exponential pressure profile from Holland (1980):

$$p(r) = p_0 + \sum_{i=1}^n dp_i e^{-\left(\frac{Rp_i}{r}\right)^{B_i}}$$

where

n = number of components

dp_i = pressure anomaly for the i 'th component

R_{pi} = scale radius for the i 'th component

B_i = Holland's B coefficient for the i 'th component

p_0 = central pressure

The model is driven from parameters that are derived from data in meteorological records and the ambient pressure field. The entire wind field history is computed from knowledge of the variation of those parameters along the storm track by computing solutions, or so-called "snapshots", on the nested grid as often as is necessary to describe different stages of intensity. The entire time history is then interpolated from the snapshots. The snapshot input parameters to TC96 are shown in Table 1.

Table 1. Model parameters for TC96.

Parameter	Description
V_{spd}, V_{dir}	speed and direction of vortex motion
V_{gs}, D_{gs}	equivalent geostrophic flow of the ambient PBL pressure field in which the vortex propagates
D_p	total storm pressure anomaly
dp_1	pressure anomaly associated with the first component of the exponential radial pressure profile
R_{p1}, R_{p2}	scale radii of the up to two components of the exponential radial pressure profile
B_1, B_2	Holland's profile peakedness parameter for each component

The model was originally validated against winds measured in several ODGP storms. It has since been applied to nearly every recent hurricane to affect the United States offshore area, to all major storms to affect the South China Sea since 1945, and to storms affecting many other foreign basins including the Northwest Shelf of Australia, Tasman Sea of New Zealand, Bay of Bengal, Arabian Sea and Caribbean Sea. Comparisons with over-water measurements from buoys and rigs support an accuracy specification of ± 20 degrees in direction and ± 2 meters/second in wind speed (1-hour average at 10-meter elevation). Many comparisons have been published (see e.g., Ross and Cardone, 1978; Cardone and Ross, 1979; Forristall *et al.*, 1977; 1978; 1980; Cardone and Ewans, 1992; Cardone and Grant, 1994).

The wind model is free of arbitrary calibration constants that might link the model to a particular storm type or region. For example, differences in latitude are handled properly in the primitive equation formulation through the Coriolis parameter. The variations in structure between tropical storm types manifest themselves basically in the characteristics of the pressure field of the vortex itself and of the surrounding region. The interaction of a tropical cyclone and its environment, therefore, can be accounted for by a proper specification of the input parameters. The assignable parameters of the planetary boundary layer (PBL) formulation, namely planetary boundary layer depth and stability, and of the sea surface roughness formulation, can safely be taken from studies performed in the Gulf of Mexico, since tropical cyclones world-wide share a common set of thermodynamic and kinematic constraints.

3. Wind WorkStation

The Wind WorkStation (WWS) is a graphical analysis tool developed in 1995 for the analysis of marine surface wind fields. The WWS was originally developed for the analysis of extra-tropical systems, but it has been extended to the analysis of tropical wind fields as well. Details on the use and objective analysis algorithm used in the WWS can be found in Cox *et al.* (1995).

The purpose of the WWS in tropical wind field generation is two-fold: First, the WWS can be used to assimilate marine surface, aircraft, and satellite observations into a tropical wind field. Where high-quality aircraft reconnaissance data are available, the WWS can be used as a direct analysis tool much in the same way as the Wind Analysis Distributed Application (WANDA) system developed by the National Hurricane Research Division (HRD) of NOAA (Powell, *et al.* 1998). Aircraft winds are reduced to the surface using a method described by Powell and Black (1990), and used directly to produce a snapshot wind field. In the absence of aircraft data, or as a supplement to the reconnaissance observations, wind fields from the tropical wind model are included in the WWS to define the tropical winds. The second purpose of the

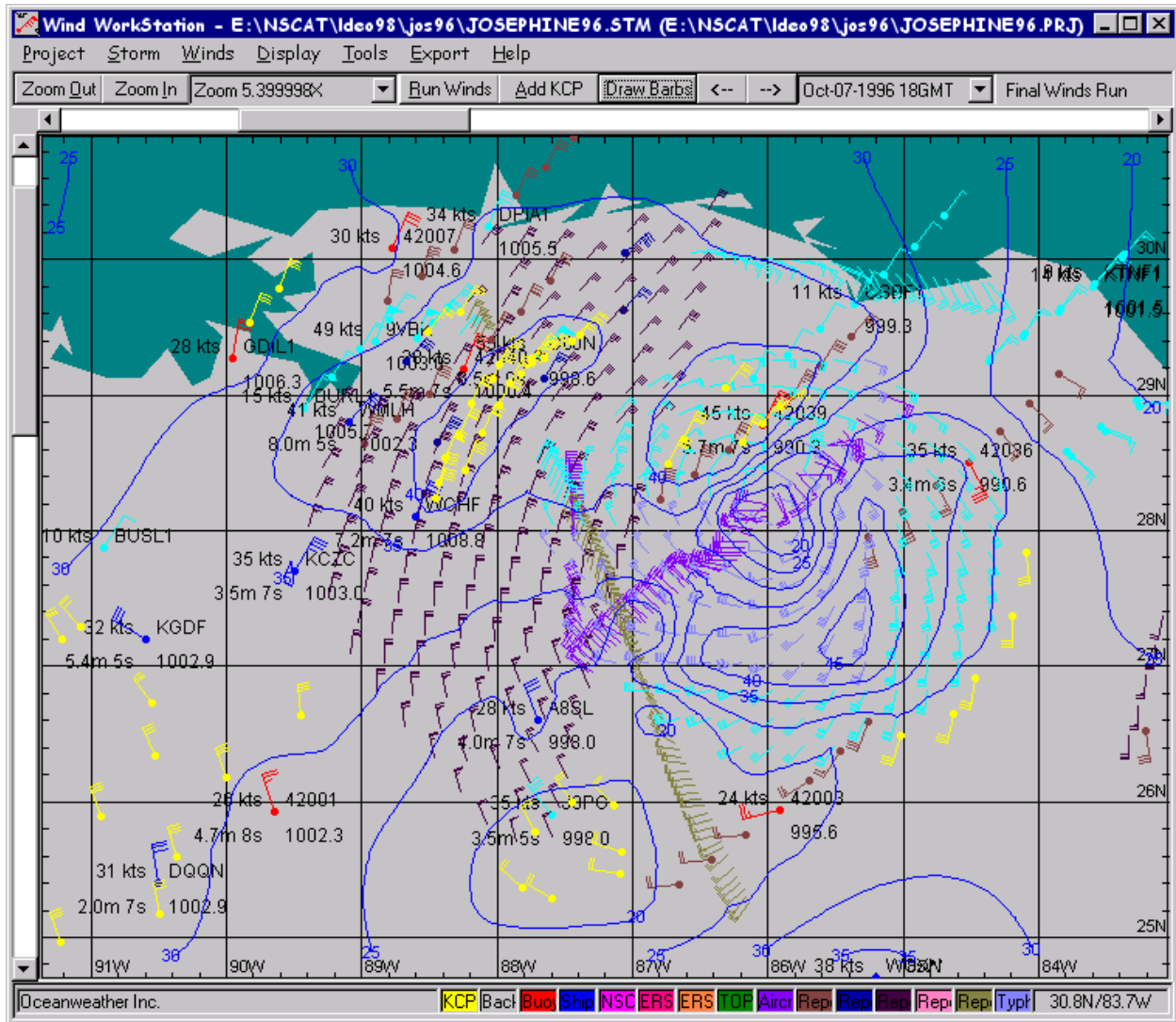


Figure 1. Wind WorkStation analysis of Hurricane Josephine (1996) valid for October 7th, 1996 at 18 GMT. Winds shown in knots, some wind inputs have been repositioned (with respect to Josephine) to synoptic time.

WWS is to blend the tropical winds with the synoptic-scale atmospheric flow to produce a basin-wide wind field for use in wave modeling. Figure 1 shows a WWS analysis of hurricane Josephine (1996) in the Gulf of Mexico. The analysis is a blend of buoy and ship winds, TOPEX altimeter winds, NSCAT scatterometer winds, TC96 model inputs, NOAA reconnaissance winds, and analyst's input.

4. Methodology

4.1 General Approach

The approach for developing tropical wind fields in both a hindcast and forecast mode is essentially the same. The relative storm motion (V_{spd} , V_{dir}) and intensity (D_p) are taken directly from best track data or from forecasts issued by warning centers such as the Tropical Prediction Center (TPC) and Joint Typhoon Warning Center (JTWC). The geostrophic flow of the ambient PBL pressure field in which the vortex propagates (V_{gs} , D_{gs}) can be estimated from

surface analyses. The remaining model parameters, the scale radii of the exponential radial pressure profile (R_{p1} , R_{p2}) and Holland's B parameter (B_1 , B_2), are the most difficult to determine. Except in cases where high quality aircraft reconnaissance indicate otherwise, typically only the single-exponential cases (R_{p1} , B_1) are considered.

In the case of aircraft reconnaissance, the surface pressure profile (reduced from flight level) can be used to fit an R_{p1}/B_1 curve to the data. Such a methodology is outlined in section 4.2. Otherwise, either wind radii information or actual wind measurements can be used to determine the R_{p1}/B_1 model parameters in an "inverse modeling" sense. A database of more than 30,000 iterations of the TC96 model runs were compiled by varying the parameters found in Table 2. Output from each model solution was saved for parameters listed in Table 3.

Table 2. Value of input parameters used in TC96 database.

Input Parameter	Value
Latitude	20 degrees
V_{spd} , V_{dir}	stationary
V_{gs} , D_{gs}	stationary
D_p	2 to 120 mb in 2 mb increments
R_p	5 nmi to 120 nmi in 4 nmi increments
B	1 to 2.5 in 0.1 increments
H	500 m (boundary layer depth)
Temperature Difference	-2 C (air-sea temperature)

Table 3. Saved output in TC96 database.

Output Parameter
Maximum surface wind
Radius of maximum wind
Azimuthally averaged wind speed in 5 nm bins
Radius (maximum) of 35 knot winds
Radius (maximum) of 50 knot winds

Once the model inputs are determined and the model run, the winds surrounding the center (typically within 180 nmi) are brought into the WWS. The model winds are then compared to the available *insitu*, satellite, and aircraft wind observations. In a hindcast mode, it is common to iterate the model inputs based on the measured winds. Once the model winds have been finalized, they are blended into the surrounding synoptic wind field using selective deletion of peripheral model inputs and the use of kinematic control points (KCPs) which are highly weighted winds added by the analyst for use in the objective analysis.

4.2 Model Inputs Derived from Aircraft Reconnaissance

When available, aircraft reconnaissance can be used to fit the pressure profile directly. Currently, aircraft reconnaissance is only available in the North Atlantic. Historically, a large database of aircraft data is also available for the North Pacific (JTWC discontinued aircraft reconnaissance 1986). In real time, typically vortex and supplementary vortex messages are available, while high-resolution observations (every 30 seconds or 1 minute) are available for hindcast studies. Aircraft pressure and wind measurements taken at flight level are reduced to the surface using techniques described by Jordan (1958) and Powell and Black (1990). Recent development of the GPS Dropwindsonde (Hock and Franklin, 1999) not only promises to measure the 10 meter surface wind directly, but to sample the entire wind shear profile which may lead to better adjustment procedures for reducing flight level winds.

Figure 2 shows a sample fit of the real-time aircraft reconnaissance estimated pressures during Hurricane Dennis (1999). The upper left panel shows the supplementary vortex message winds plotted as distance from the center of Dennis (center position computed from closest vortex messages interpolated to wind observation time). The map in the upper right shows the track of Dennis from vortex messages with wind barbs (in knots) indicating the adjusted surface ten-minute wind. The lower

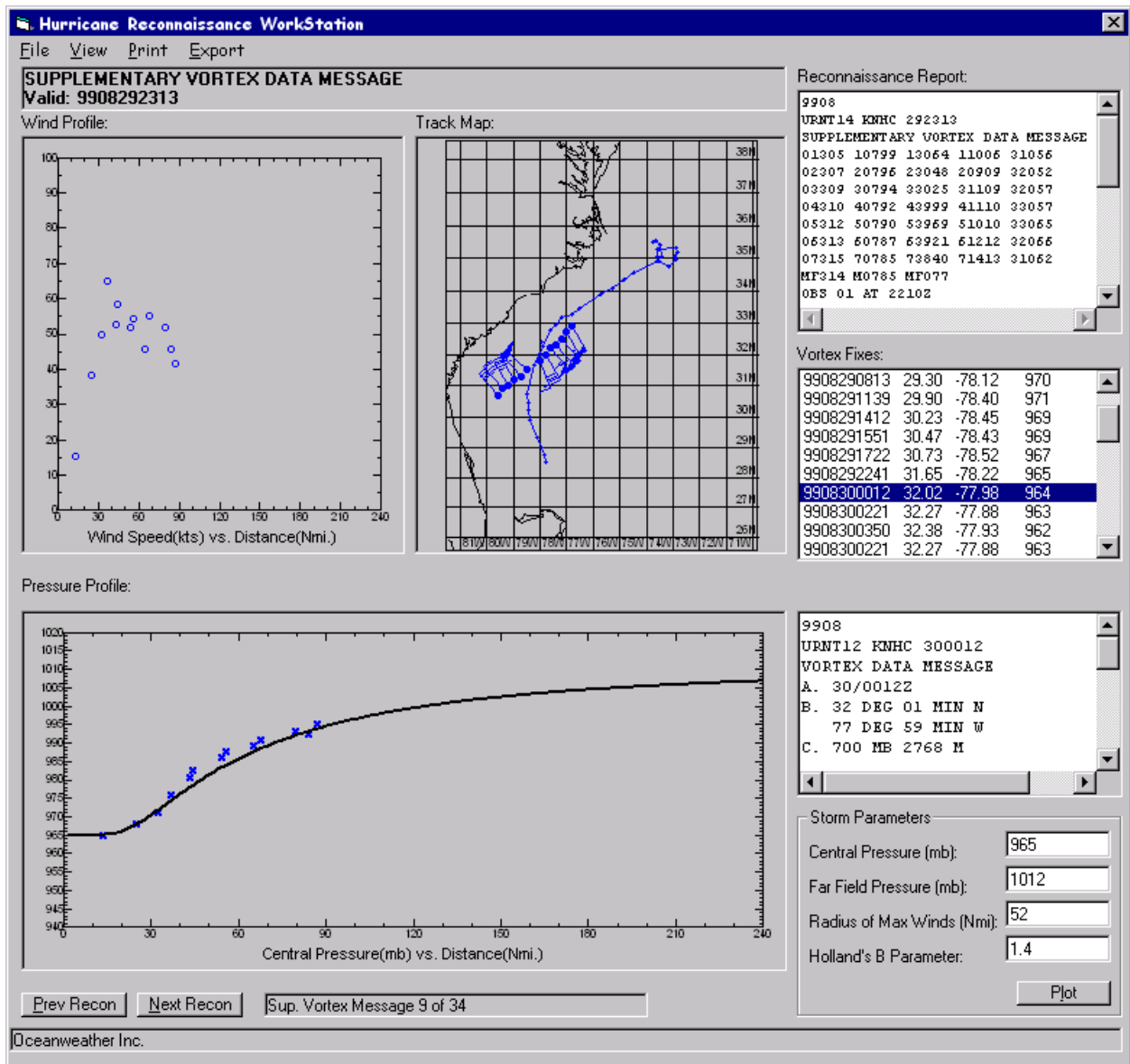


Figure 2. Real-time pressure profile fit to aircraft reconnaissance surface pressures reduced from flight level.

panel shows the reduced aircraft surface pressures with a profile fit. The fit profile of $D_p=47$ (1012-965), $R_p=52$ and $B_1=1.4$ corresponds to a TC96 model maximum one-minute wind of 88.4 knots. The closest vortex message indicates that a surface wind of 86 knots (one-minute) was observed at this time.

4.3 Model Inputs Derived from Official Forecast Guidance Wind Radii

Official forecasts from both TPC and JTWC for global tropical systems include forecast track, intensity and radii of 35 and 50 knots. It is desirable for an operational wind/wave forecast to as closely match as possible the official forecasts, both for consistency and for derivative

forecast products which are based on an individual warning center's error statistics (such as a probabilistic wind/wave forecast).

To make use of the official forecast parameters, the TC96 database is first searched for all model solutions with a D_p matching the official forecast intensity with a maximum wind solution ± 2 m/s from the adjusted forecast intensity. The forecast intensity is adjusted for forward speed since the database assumes a stationary system. The resulting model solutions are then sorted by the radii of 50 (preferred) or 35 knots, and the model parameters are then interpolated from the closest 2 snap inputs. In cases where the tropical wind radii in a particular quadrant are enhanced by a synoptic-scale feature, the non-affected quadrant is used to determine the snap parameters and synoptic enhancement is modeled through the WWS.

This wind radii technique was recently applied in a hindcast mode. The GROW2000 (Global Reanalysis of Ocean Waves) project involved hindcasting the global ocean for the period 1979 to 1998. While the resolution of the global model (.625 by 1.25 degrees) was relatively coarse for tropical modeling, tropical systems were added to base GROW2000 wind fields to better predict the swells generated by tropical systems. A database of wind radii analyzed by JTWC was obtained for much of the Northern and Southern Pacific Oceans and was used to determine TC96 model parameters (Atlantic systems had already been analyzed in a previous project). The resulting tropical winds were more accurate than could be expected from using a simple climatological R_p/B_1 ratio since they reflected an individual storm's wind radii as analyzed by JTWC.

4.4 Model Inputs Derived from QUIKSCAT Wind Measurements

The global coverage and wide-swath of surface marine winds available from the QUIKSCAT scatterometer make this instrument well suited for the detection and analysis of tropical cyclone winds. However, this instrument suffers from

both rain contamination and model function saturation that limits its use in winds over 20 m/s. Recent studies (Jones *et al.* 1999 and Cardone *et al.* 1999) indicate that a neural net algorithm for tropical cyclone winds may extend this limit to 25 m/s, but it is not yet clear that wind speed above 30 m/s will be retrievable.

While the radii of 35 knot winds can be determined from QUIKSCAT data (and perhaps someday the 50 knot radii) and the methodology in section 4.2 applied, the wide swath data make it possible to fit the model winds across the entire wind profile sampled by QUIKSCAT. Figure 2 shows QUIKSCAT wind measurements vs. distance from the center of hurricane Floyd (1999) for one pass. The thick line is the azimuthally averaged QUIKSCAT wind in 5 nmi bins. The dashed lines are a family of TC96 model solutions for a given D_p where $B_1 = 1.00$ (representing $1/15^{\text{th}}$ of the total possible combinations in the TC96 database for this D_p). While the range of maximum winds for this D_p / B_1 combination has a 5 m/s range, the wind speed difference outside the radius of maximum winds is as much as 25 m/s.

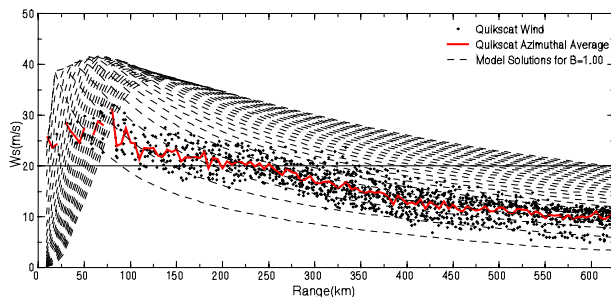


Figure 3. Family of TC96 model solutions (dashed) for $D_p=90$, $B_1 = 1.00$ vs. azimuthally averaged QUIKSCAT data (solid) during hurricane Floyd (1999).

Figure 4 shows a best root mean squared (RMS) fit (left) of a TC96 database solution to the azimuthally averaged QUIKSCAT data for September 14th at 12 GMT. Only azimuthally averaged QUIKSCAT winds below 20 m/s were considered in this fit to minimize the influence of model retrieval underestimation. Twenty-two snapshots were derived during the lifetime of

Floyd using this methodology where sufficient QUIKSCAT was available. The resulting tropical wind field, when compared directly to QUIKSCAT observations, had a mean difference of .81 m/s with a scatter index (SI) of .23 and correlation coefficient of .87.

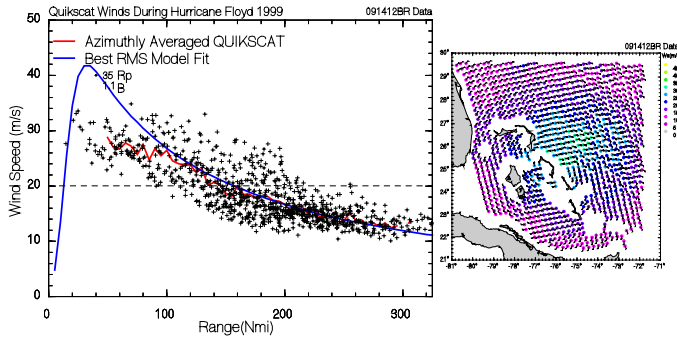


Figure 4. Best RMS fit to QUIKSCAT azimuthally averaged winds on September 14th 12 GMT.

5. Case Study during Hurricane Floyd (1999)

Hurricane Floyd is an excellent test case for determining TC96 parameters from scatterometer measurements. The QUIKSCAT data allowed the selection of 22 snapshots during the lifetime of Floyd where there was sufficient data in all quadrants. These snapshots, along with the best track from NHC were used to construct the tropical wind field for Floyd without the direct use of reconnaissance data (although reconnaissance data was used by NHC to determine the track and intensity).

During Floyd, HRD produced 24 wind field snapshots using the WANDA system. While the HRD winds do not constitute an absolute standard for verification, they do provide a measure of the success of the QUIKSCAT inverse modeling technique. The TC96 model winds were compared to the HRD winds at the time of the HRD analyses. Overall, the TC96 model winds were biased high by 2.79 m/s with a SI of .17 and correlation coefficient of .92. Wind directions were biased by -5.6 degrees. These statistics indicate a close statistical match between the QUIKSCAT derived inverse model

winds and the HRD aircraft derived winds. Differences within a given snapshot occasionally display large spatially coherence differences. These differences may arise from a number of causes including: (1) failure of the TC96 model to simulate smaller scale spiral bands which are sensed by the aircraft; (2) HRD wind errors in storm quadrants not probed by the aircraft and (3) slight positioning errors in wind field features which have been qualitatively well modeled by both wind fields.

The HRD and TC96 wind fields were both imbedded into a synoptic-scale wind field using the WWS, and run through a .25-degree 3rd generation wave model adapted to the Western North Atlantic. A comparison of the winds and waves during Floyd at NOAA buoy 41002 (Figure 5) show similar characteristics from the HRD and TC96 winds and waves. There is a slight underestimation of the winds and waves by the HRD winds and a slight overestimation by the TC96 model at this buoy. Overall, both hindcasts verify well. Wind comparisons to buoy 41010 (not shown), which was closest to the center of Floyd, show that the TC96 model winds tracked the measured wind speed very closely, except at the peak of the storm. The storm peak was overestimated by 7.5 m/s. The overestimation occurs when the modeled waves were greater than 9 meters (wave measurements at 41010 were not available). Given the extreme waves that the buoy likely encountered, coupled with the higher estimation of maximum winds by NHC (Table 4), it is likely that the buoy measurements are biased low and may have pulled down the peak winds in the HRD analysis which assimilated the buoy winds.

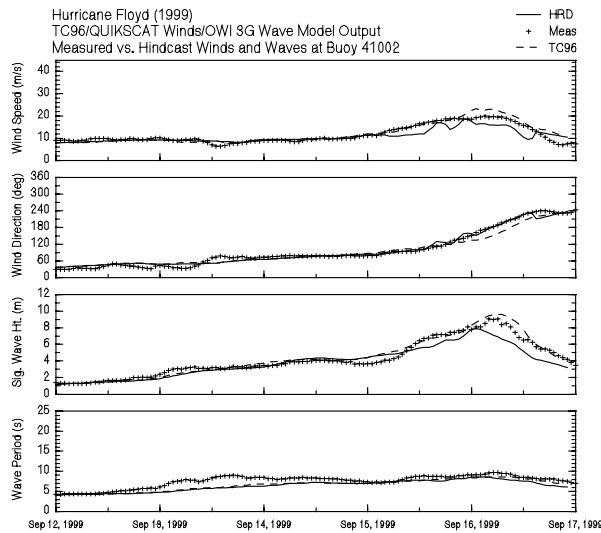


Figure 5. Comparison of wind and waves from HRD (solid) and TC96 (dashed) at Buoy 41002.

Table 4. Comparison of peak 10-minute, 10 meter wind speeds (m/s) during Floyd.

TC96	HRD	Buoy	NHC Best Track
43.0	38.0	35.5	41.2

Overall, the TC96 model winds during Floyd show very good skill when compared directly against QUIKSCAT, HRD, and buoy winds and indirectly compared to buoy wave measurements. Given the global coverage of QUIKSCAT, this technique shows promise for the increased skill of tropical wind fields where aircraft reconnaissance is not available.

6. Conclusion

This paper describes the system and techniques used to specify the surface wind field in tropical cyclones. The system is designed about the TC96 model, a well-proven tool that has been applied and validated in tropical basins worldwide. Methodologies applicable in both hindcasting and forecasting settings have been presented and have shown to be skillful when compared to measured wind and wave datasets.

References

Cardone, V. J., W. J. Pierson, and E. G. Ward, 1976. Hindcasting the directional spectra of hurricane generated waves. *J. of Petrol. Technol.*, 28, 385-395.

Cardone, V. J. and D. B. Ross, 1979. State-of-the-art wave prediction methods and data requirements. *Ocean Wave Climate* ed. M. D. Earle and A. Malahoff. Plenum Publishing Corp., 1979, 61-91.

Cardone, V.J., C.V. Greenwood, and J.A. Greenwood, 1992. Unified program for the specification of hurricane boundary layer winds over surfaces of specified roughness. Final Report. Contract Report CERC-92-1. Dept. of the Army, Waterways Experiment Station, Vicksburg, MS.

Cardone, V.J. and K.C. Ewans. 1992. Validation of the hindcast approach to the specification of wave conditions at the Maui location off the west coast of New Zealand. Preprints of the Third International Workshop on Wave Hindcasting and Forecasting, May 19-22, 1992, Montreal, Quebec, 232-247.

Cardone, V.J., A.T. Cox, J.A. Greenwood and E.F. Thompson, 1994. Upgrade of Tropical Cyclone Surface Wind Field Model Misc. Paper CERC-94-14, US Army Corps of Engineers.

Cardone, V.J. and C.K. Grant, 1994. Southeast Asia Meteorological and oceanographic hindcast study (SEAMOS). OSEA 94132. 10th Offshore Southeast Asia Conference, 6-9 December, 1994.

Cardone, V.J., A.T. Cox, W.J. Pierson, W.B. Sylvester, W.L. Jones and J. Zec, 1999. NASA Scatterometer High Resolution Winds for Hurricane Lili. IEEE 1999 International Geoscience and Remote Sensing Symposium (IGARRS'99) 28 June-2 July, 1999, Hamburg.

Chow, S. H., 1971. A study of the wind field in the planetary boundary layer of a moving tropical cyclone. Master of Science Thesis in

Meteorology, School of Engineering and Science, New York University, New York, N.Y.

Cox, A.T., J.A. Greenwood, V.J. Cardone and V.R. Swail, 1995. An Interactive Objective Kinematic Analysis System Fourth International Workshop on Wave Hindcasting and Forecasting. October 16-20, 1995. Banff, Alberta, Canada.

Forristall, G.Z., R.C. Hamilton and V.J. Cardone, 1977. Continental shelf currents in tropical storm Delia: observations and theory. J. of Phys. Oceanog. 7, 532-546.

Forristall, G.Z., E.G. Ward, V.J. Cardone, and L.E. Borgman. 1978. The directional spectra and kinematics of surface waves in Tropical Storm Delia. J. of Phys Oceanog., 8, 888-909.

Forristall, G.Z., E.G. Ward and V.J. Cardone., 1980. Directional spectra and wave kinematics in hurricanes Carmen and Eloise. 17th International Conference on Coastal Engineering, Sydney, Australia.

Jones, L.W., V.J. Cardone, W.J. Pierson, J. Zec, L.P. Rice, A.T. Cox and W.B. Sylvester, 1999. NSCAT High Resolution Surface Wind Measurements In Typhoon Violet J. Geophys. Res. (Oceans), vol. 104, no.C5, pp. 11247-11259, May 15, 1999.

Jordon, C.L., 1958. Estimation of Surface Central Pressures in Tropical Cyclones from Aircraft Observations. Bul. of Amer. Met. Soc. 39, pp. 345-352.

Hock, T.F., and J.L. Franklin, 1999: The NCAR GPS dropwindsonde. Bull. Amer. Meteor. Soc., 71, 1410-1428.

Holland, G. J., 1980. An analytical model of the wind and pressure profiles in hurricanes. Mon. Wea. Rev. 1980, 108, 1212-1218.

Ross, D. B. and V. J. Cardone, 1978. A comparison of parametric and spectral hurricane wave prediction products. Turbulent Fluxes through the Sea Surface, Wave Dynamics, and Prediction, A. Favre and K. Hasselmann, editors, 647-665.

Shapiro, L. J., 1983. The asymmetric boundary layer flow under a translating hurricane. J. of Atm. Sci. 39 (February).

Powell, M.D., and P.G. Black (1990). The relationship of hurricane reconnaissance flight-level wind measurements to winds measured by NOAA's oceanic platforms. J. Wind Engrg. and Industrial Areodynamics, 36, 381-392.

Powell, M.D., S.H. Houston, L.R. Amat and N. Morisseau-Leroy, 1998. The HRD real-time hurricane wind analysis system. J. of Wind Eng. and Ind. Areodynamics. 77&78, pp. 53-63.

Thompson, E. F. and V. J. Cardone, 1996. Practical modeling of hurricane surface wind fields. ASCE J. of Waterway, Port, Coastal and Ocean Engineering. 122, 4, 195-205.